THE UNIVERSITY OF MICHIGAN

COLLEGE OF ENGINEERING
DEPARTMENT OF NAVAL ARCHITECTURE
AND
MARINE ENGINEERING

Observations of Unsteady Airfoil Flows

BRUCE A. NELSON
MICHAEL B. WILSON
FINN C. MICHELSEN

December 1965

ANN ARBOR

THE UNIVERSITY OF MICHIGAN

COLLEGE OF ENGINEERING
DEPARTMENT OF NAVAL ARCHITECTURE
AND
MARINE ENGINEERING

Final Report

Observations of Unsteady Airfoil Flows

Bruce A. Nelson
Michael B Wilson
Finn C. Michelsen

This Research Was Sponsored By

Panel H-8 (Hydroelasticity) of The Society of
Naval Architects and Marine Engineers

December, 1965

ACKNOWLEDGEMENT

The objectives of this pilot study could not have been accomplished without the services of Mr. Otto Scherer. He was largely responsible for making the special laboratory setup available for this project following a gust study for which it was originally built. His principle contribution, however, is the design and construction of the foil in such a way that a sufficient quantity of "smoke" would be emitted into the boundary layer at the correct relative velocity. Mr. Scherer's service to this study was unfortunately terminated because of graduation.

TABLE OF CONTENTS

Page

ACKNOWLEDGEMENT.......... ii

LIST OF FIGURES.......... iv

I. ABSTRACT.......... 1

II. INTRODUCTION.......... 2

III. DISCUSSION AND RESULTS.......... 5

IV. DESCRIPTION OF EXPERIMENTAL TECHNIQUE.......... 8

A. Experimental Apparatus.......... 8

Track and Carriage System.......... 8
Carriage Propulsion.......... 8
Model Description.......... 11
Gust Simulation.......... 11

B. Procedure for Photographic Work.......... 26

V. CONCLUSIONS AND RECOMMENDATIONS.......... 27

VI. REFERENCES.......... 28

VII. APPENDIX.......... 29

LIST OF FIGURES

Figure		Page
1	Test Airfoil Section..............................	9
2	Sample of Aerodynamic Characteristics for Tested Foil..	9
3	Schematic of the Track and Carriage System..........	10
4	Model Accelerating Mechanism.........................	12
5	Views of the Wing Model Showing the Smoke Generation Device..................................	13
6	View of the Mounted Foil, the Carriage, and the Track...	14
7	Velocity Profile of Gust at 12" from Nozzle.........	15
8	Photographic Results................................	16-17
9	Photographic Results................................	18
10	Photographic Results................................	19-21
11	Photographic Results................................	22-25
A-1	Definition of Angles Θ_o and β_o.....................	30
A-2	Four Regions of the Problem for the "Broken Line Airfoil"......................................	31
A-3	"Flat Plate" Jet Deflection Phenomenon..............	34

I. ABSTRACT

This report describes a pilot study investigation of two-dimensional unsteady flow about an airfoil passing through a narrow (or gust). Although the results are primarily photographic records of the flow observed, there are also included comments and sample calculations taken from existing and slightly extended theories of unsteady airfoil behavior. Such work appears in the appendix of the report.

One of the main items of interest was the particular flow phenomena around the trailing edge -- specifically the visualization of the Kutta condition. In this conjunction, medium speed and "Fastax" films were made and should accompany the still photos contained in the report.

II. INTRODUCTION

The study of unsteady flows about airfoils is not in a satisfactory state of development neither analytically nor experimentally. This appears to be particularly true for foils experiencing the effects of very thin gusts (the width being smaller or roughly comparable to the chord length). "Gusts" are cross flows of a uniform or non-uniform character imposed on the steady stream flow over an airfoil. Allowing that the problem of unsteadiness is in itself difficult to attack in an unrestricted fashion, there may be, moreover, reasons to place question marks on certain assumptions that have remained for a long time unassailable. In particular, the Kutta condition is one of the essential building blocks of an airfoil theory which in the future may need to be improved in order to answer demands imposed by unsteadiness.

This problem is clearly pertinent to extending our knowledge about the time variation of lift and moment on propeller blades in ships' wakes, the performance of rudders or fins in the presence of cross flows, and the behavior of hydrofoils in unsteady motions.

It is well known that the build up of viscous effects in the boundary layer will reach rather significant proportions along a foil. There have been numerous pervious speculations about the possibility of a "wandering" point of separation for the flow in the immediate neighborhood of the trailing edge. The presence of large viscous influences and the problems of unsteady exterior flows are probably in truth interacting with one another. We may easily speculate about unsteady changes in lift being brought about strictly by "non-potential" alterations in the actual foil circulation. If such is the case, the Navier-Stokes equations might reveal some sort of periodic movement of the separation point to either side of the steady state location. Moreover, these vibrations could very well be forced by unsteady flows about the lifting body involved. Study of the viscous equations of motion could be the theoretical avenue for the problem, but it would clearly be fraught with exceedingly difficult problems.

Even for the case of simple steady flow over airfoils, the build up of the boundary layer is enough to affect the experimental lift behavior. Pinkerton in Reference (5) has shown that experimental data and suitably modified potential flow relations can successfully account for discrepancies between experimental pressure distributions and those calculated from potential flow. The idea he proposes is to allow the effective shape of the profile to be changed by the influences of the boundary layer. Instead of using the theoretical value of circulation Γ at the given angle of attack, he calculated the effective Γ from the experimental lift $\Gamma_{exp} \doteq \frac{L_{exp}}{\rho U}$. This is tantamount to relaxing the Kutta condition, since now the factor multiplying the infinite term of the complex velocity (at the trailing edge) is non-zero. In order to avoid sudden high suction pressures due to the discontinuity, the profile shape is modified to force the factor back to zero. Admittedly artificial, the resulting alteration suggests the presence of the "virtual" profile surface where the boundary layer would be thickest. As a consequence, the resulting pressure calculations are very much improved in their agreement with the experiments. In effect, the modified procedure does satisfy the Kutta condition, but on an altered tail form from the original foil.

We may pose the question: would such a correction be relevant or worthwhile with an unsteady flow problem?

Assuming for the moment that the Kutta condition problems are of higher order, there is still another area where knowledge can be extended. Meyer in Reference (4) has given an excellent start to solutions of the "thin gust" problem. We feel that these should be investigated at great length.

This paper reports only preliminary photographic records of unsteady flows. However, we believe that the background commentary on the Kutta condition and the thin gust problem place the work in the proper context, and point to areas toward which future investigations should aim.

III. DISCUSSION AND RESULTS

Being a pilot study, this report contains primarily photographic flow visualizations. Included here are photos which are representative samples of the strobe flash Polaroid films, and also a selected series of individual stills gleaned from the high speed motion pictures. These results are intended to be further augmented by the actual motion picture films themselves which were taken at camera speeds 300 and 1260 frames per second.

Three complete series of the best of the flash pictures are contained in Figs. 8 a-e; Figs. 9 a-g; and Figs. 10 a-g. Two of these illustrate typical flow behavior with smoke being released into the pressure side of the foil. The third set demonstrates the case of smoke vented into the stream on the suction (back) side. It may be noted here that several other port openings were also tried: one near the leading edge stagnation region, and the other clear aft at the trailing edge. Neither of these latter configurations provided smoke trails of sufficient clarity compared with those shown here.

In general, all the photographs concentrate on showing the effects of the gust on the flow around the aftermost part of the wing section, in particular around the trailing edge. This was motivated principally by our interest in the Kutta condition for foils experiencing unsteadiness.

For the first three series given here (Figs. 8, 9 and 10) the individual photos were shuttered by a switch located at one inch intervals along the track. The fourth and longer series (Fig. 11 a-v) represents a systematic selection of frames taken from one of the "Fastax" films. Complete notations of foil velocity, gust location, etc. are made in the captions of the various figures.

The narrowness of the gust in comparison with the chord length introduces some interesting unsteady flow patterns. Most noticeable of these is the rather localized effect of the gust on the smoke trail. The influence appears to be simply a jet impingement on a moving plate. In particular, notice the suggestive swirls of smoke in Figs. 8b, 8c, 8d, 8e, 9c, 9d, 9e, 9f and 9g. Such effects do not seem to be restricted to the pressure side alone. We have a hint of a similar but "reversed" effect occurring on the foil's back face in Fig. 10g.

Figs. 11 a-v show the same phenomenon as the flash photos, but with shorter intervals between successive shots.

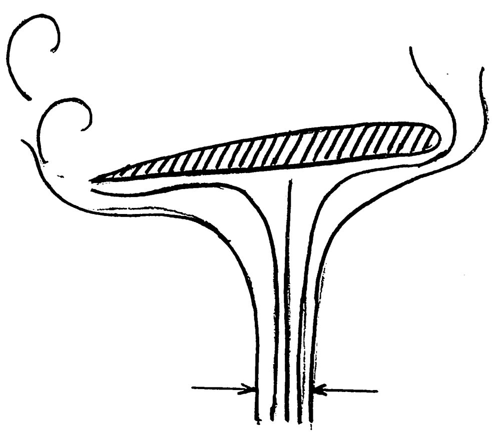

"jet impingement" flow

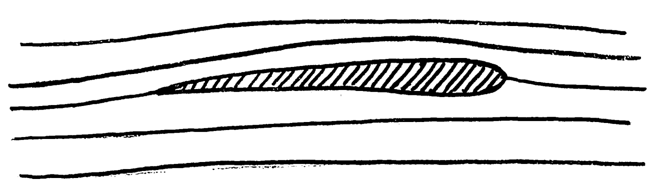

steady lifting flow

The ratios of maximum gust velocities to the foil velocities were rather extreme in the cases shown, being at the smallest $= 1/2$. Nevertheless, the effect of the narrow gusts considered here is <u>not</u> to have a large change in the relative angle of attack. Rather, the combined flows sketched above simply cause a local jet impingement with an angle other than $90°$ as shown.

Thus, the initial angle of attack of the foil is of no great consequence, except that we demand that the foil has not stalled. Meyer in Reference (4) proceeds to develop a theoretical analysis for a similar notion (see the appendix). As a consequence, it would appear that the magnitude and nature of unsteady variations of lift and moment on foils (or propeller blades) would be nearly exclusive functions of the impinging gust rather than the steady state load.

IV. DESCRIPTION OF EXPERIMENTAL TECHNIQUE

A. Experimental Apparatus

Flow visualization was made around a NACA 4412 airfoil section shown in Fig. 1. Simple aerodynamic data calculated from Reference (1) for a wing of aspect ratio: $\mathcal{R} = 3$, are contained in Figs. 2. The model used in this experimentation has a chord length $c = 1$ ft. with a span of $b = 3$ ft., and was mounted vertically on a carriage which ran along a set of three aluminum rails.

Track and Carriage System

The arrangement of the tracks and their support is shown in Figs. 3 and 3a. Mounted on a 3/4" plywood base, the track system lies at about knee height and consists of two outer channels and one inside angle. Extruded aluminum sections were used because of their smoothness and good flange tolerances.

Guided by the constraining wheel assemblies, the carriage is a 3/4" plywood chassis 18" long and 12" wide. The wheels are arranged in such a way that the only direction of free movement is along the direction of the tracks. Refer again to Fig. 3.

Carriage Propulsion

In order to accelerate the carriage to the desired speed (15-20 fps) and to contain its movement after passage beyond the test section of the track, a system of shock cords was used. These were placed in a sort of double sling shot configuration: one set to propel and the other to decelerate the carriage with its mounted foil. The

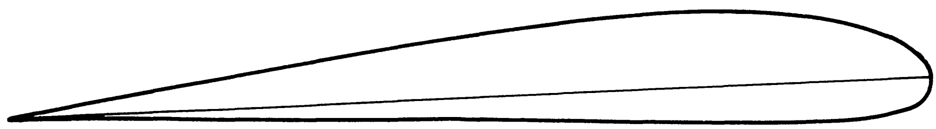

Fig. 1

Test Airfoil Section

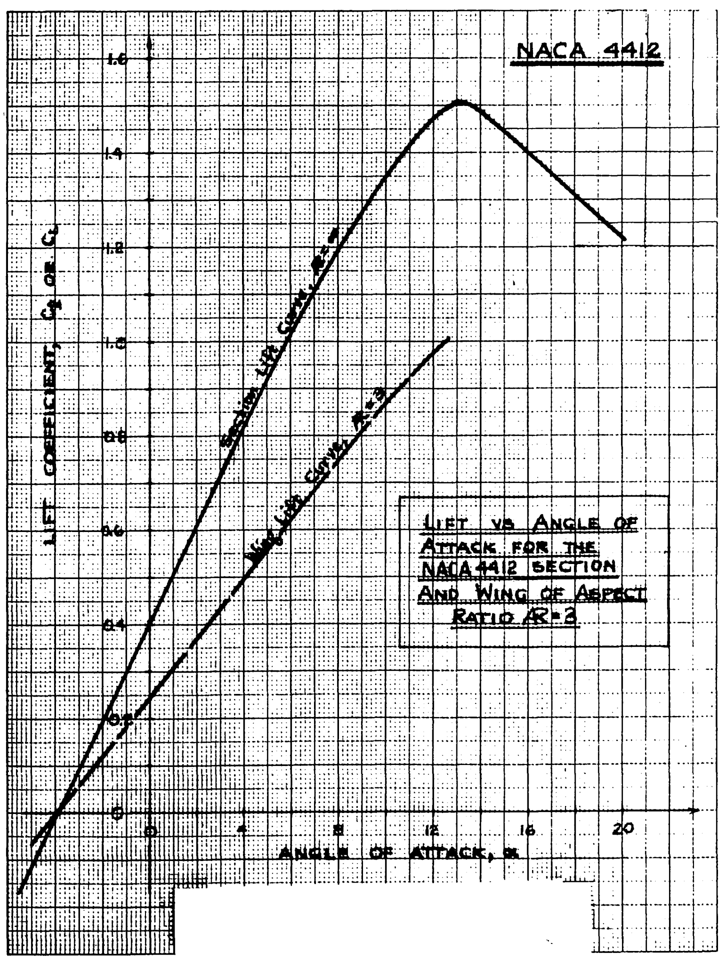

Fig. 2

Sample of Aerodynamic Characteristics for Tested Foil

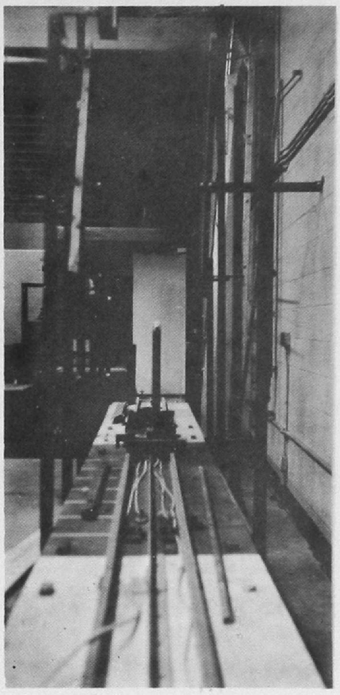

Fig. 3a

Photograph Along the Track of the Set-Up

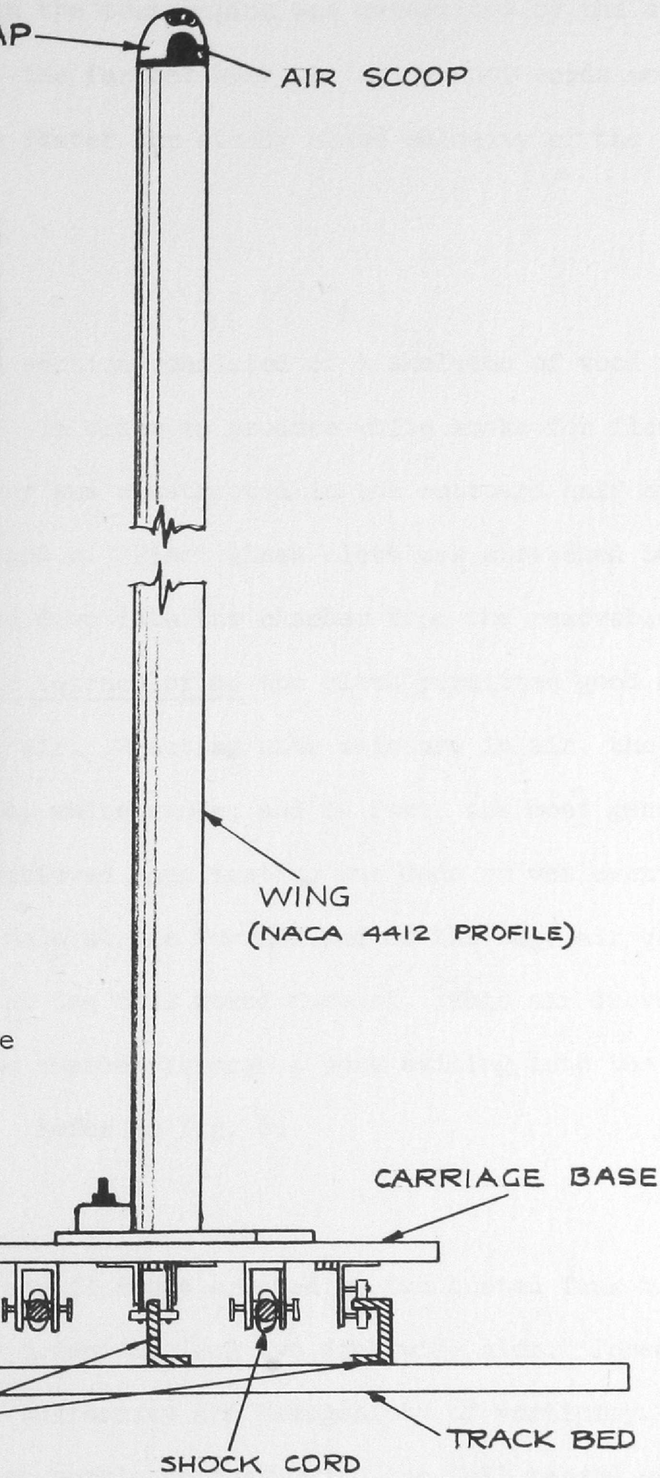

Fig. 3

Schematic of the Track and Carriage System.

speed of the wing through the test region was determined by the starting point of the carriage -- the farther back the sling shot cords were stretched initially, the faster the steady state velocity of the foil. See Fig. 4.

Model Description

The model wing section consisted of a skeleton of wood covered with a skin of aluminum. In order to produce white smoke for flow tracing, a smoke generating chamber was constructed in the outboard half of the wing. See Figs. 5 a, b and c. Fiber glass cloth was stretched between two dowel rods protruding down into the chamber from the removable cap. When soaked with titanium tetrachloride the cloth permitted good contact between the chemical and air. Reacting with moisture in air, the fluid produced billows of dense, white smoke; and in fact, the most generous supplies of smoke were achieved when testing was done on wet evenings.

By means of a hole at the forward end of the cap, air was forced into the chamber as the foil moved forward. This air drove the smoke down and out of the chamber through a port exiting into the stream flow around the section. Refer to Fig. 6.

Gust Simulation

The gust or cross flow was created by two ducted fans blowing air through a vertically oriented, long two inch wide slot. Screening was used to help improve uniformity and homogeniety of vorticity. The distance out from the gust nozzle through which the foil passed was taken at 6" and 12" respectively. Figs. 8 and 9 show the gust source at a distance of 6" and Figs. 10 and 11 illustrate the results at 12". For the

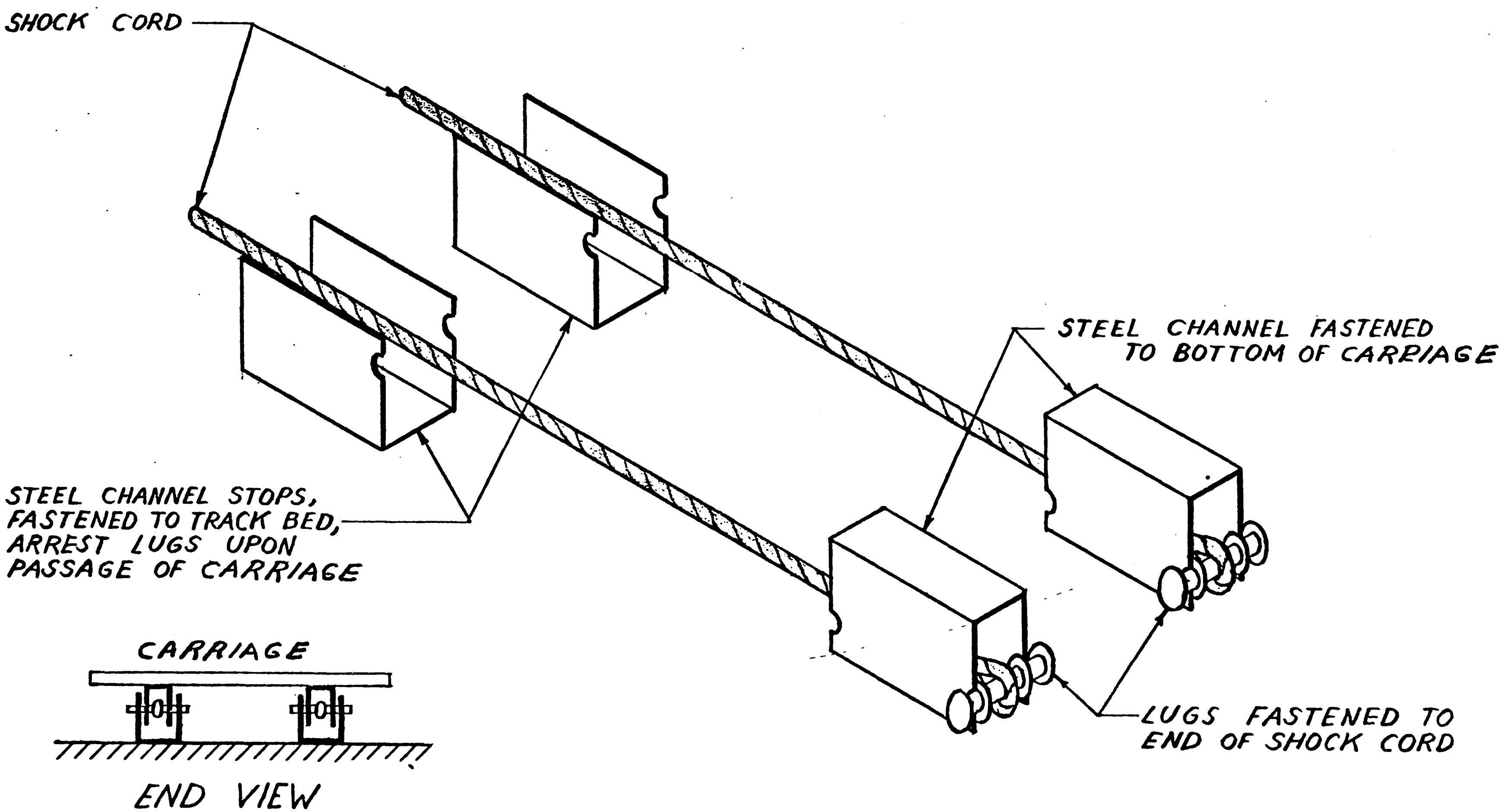

Fig. 4

Model Accelerating Mechanism

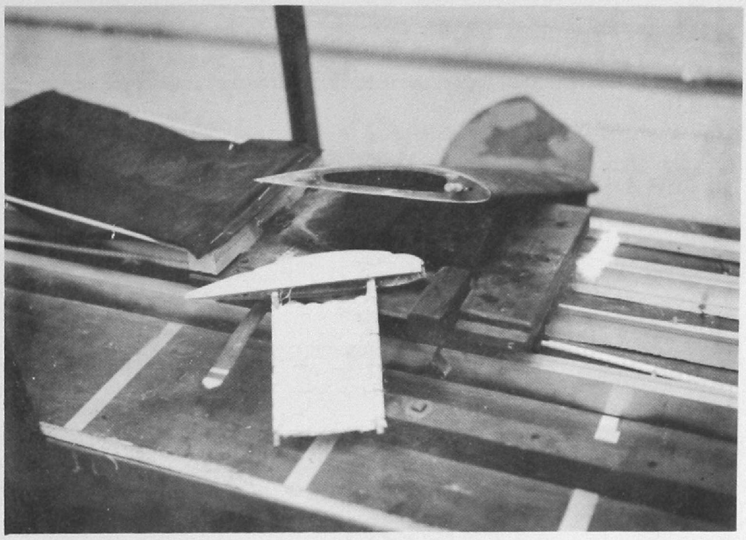

Fig. 5a.

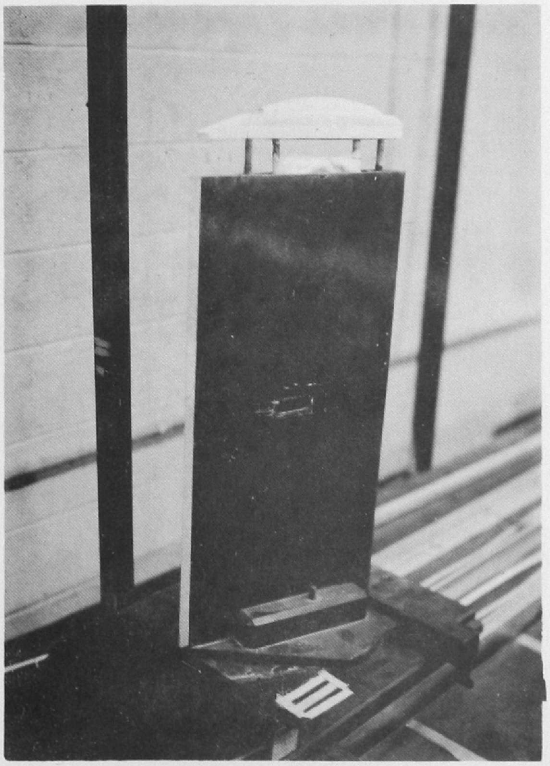

Fig. 5b

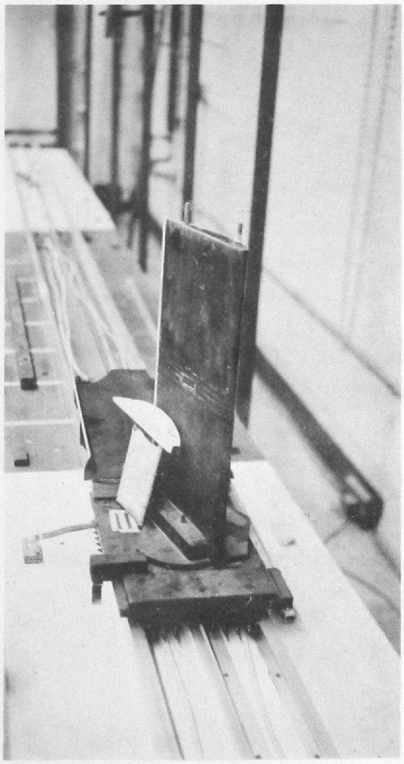

Fig. 5c.

Fig. 5

Views of the Wing Model Showing the Smoke Generation Device.

SMOKE GENERATING DEVICE

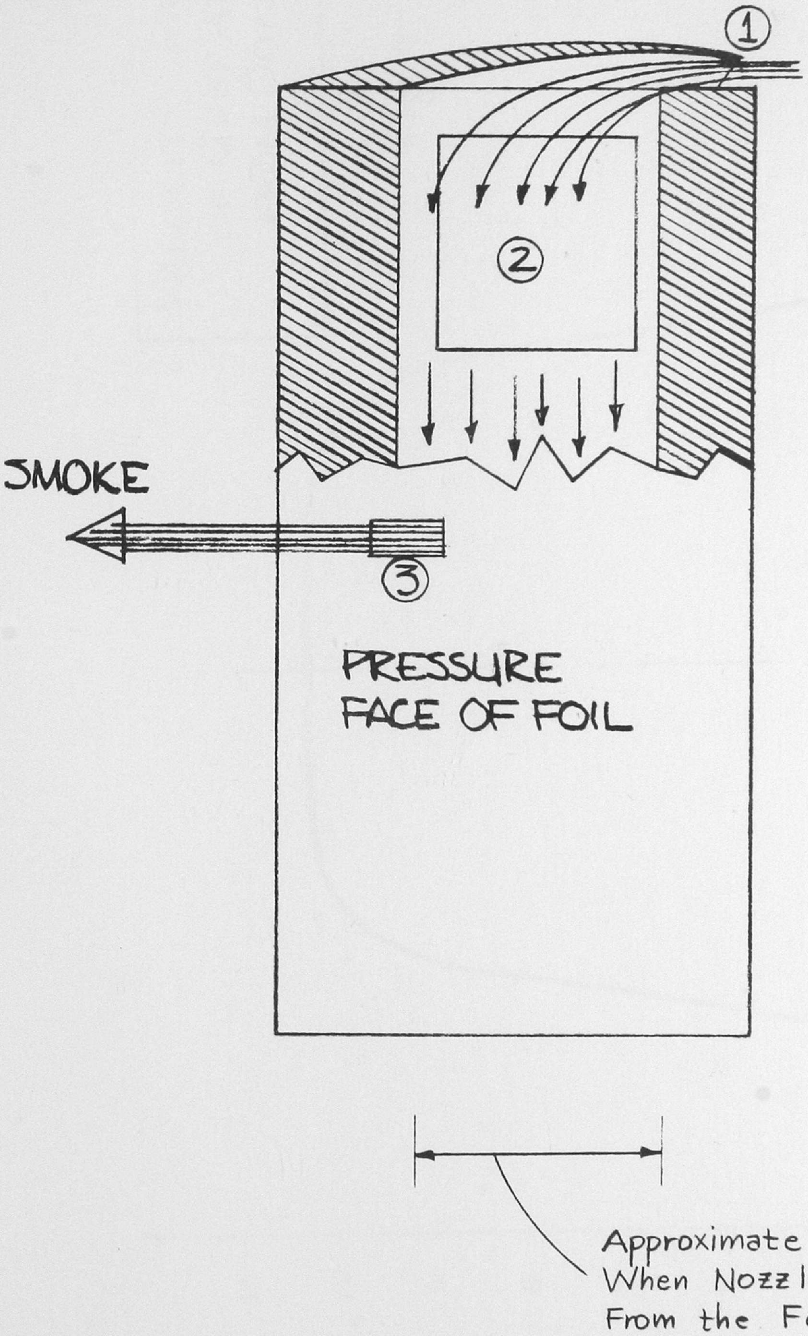

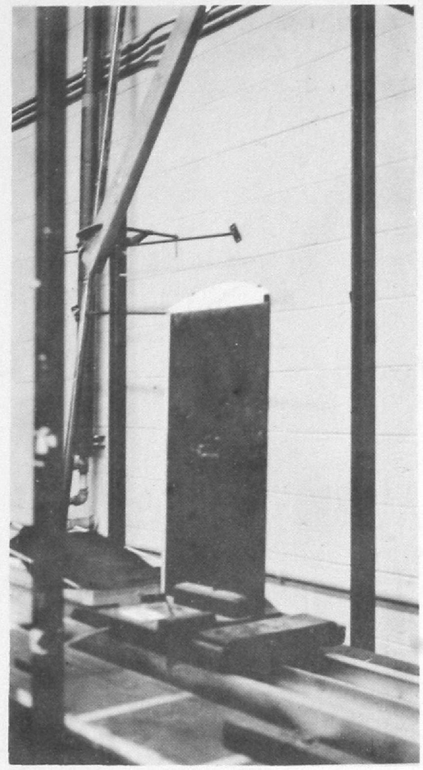

(1) : Air Scoop

(2) : Fiber Glass Cloth Soaked With Titanium Tetrachloride

(3) : Pressure Face Smoke Port

Fig. 6

View of the Mounted Foil, the Carriage, and the Track

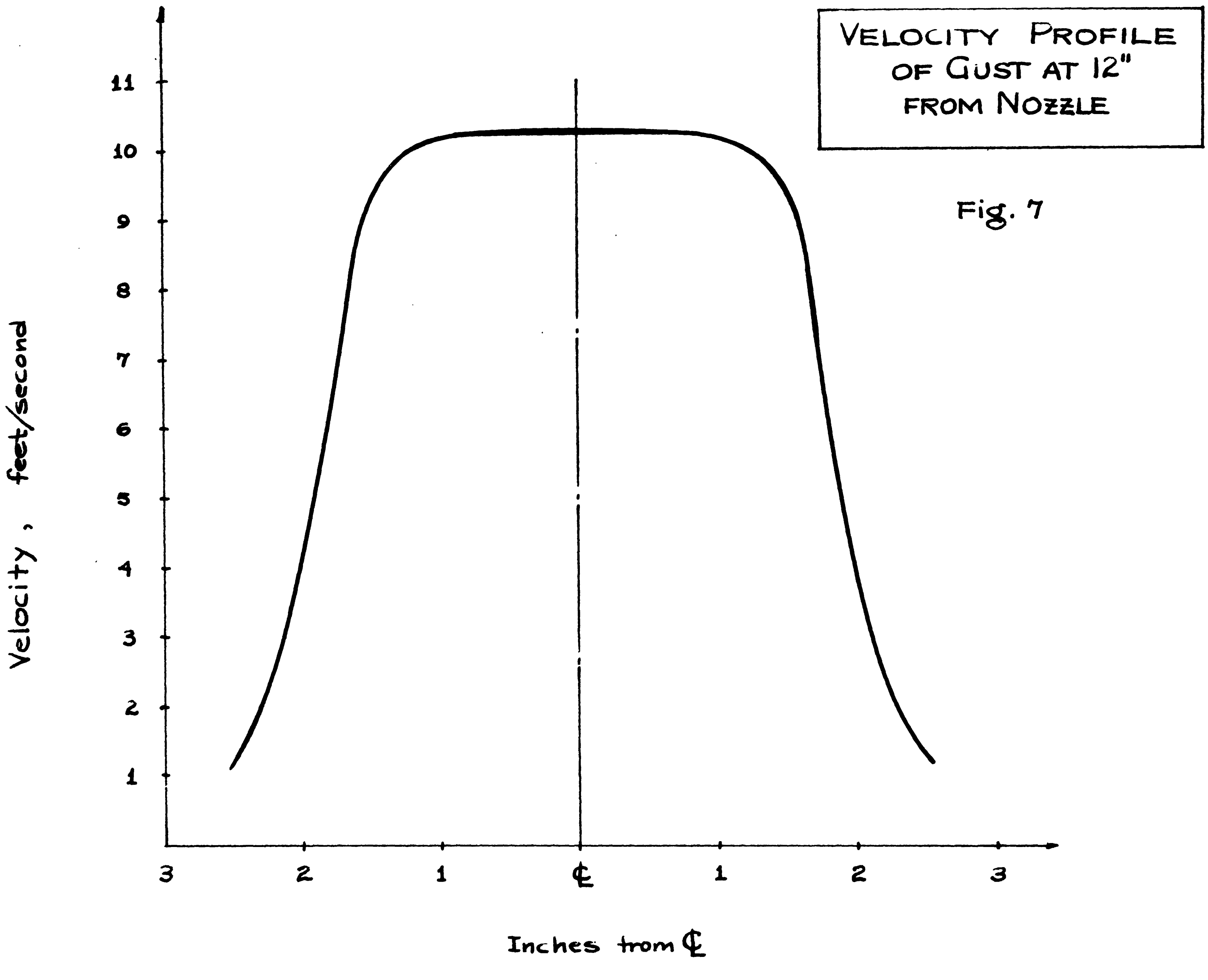
VELOCITY PROFILE
OF GUST AT 12"
FROM NOZZLE
Velocity, feet/second
11
10
9
8
7
6
5
4
3
2
1
3
2
1
℄
1
2
3
Inches from ℄

Fig. 7

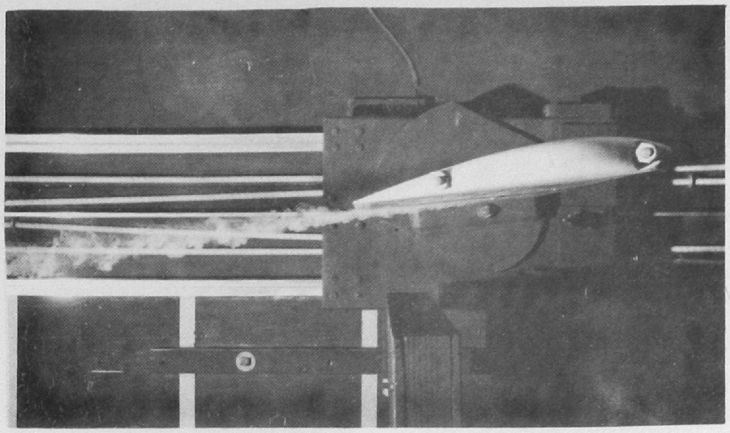

<u>Fig. 8a</u>

Foil Velocity V = 10.8 ft/sec
No Gust
Smoke from pressure face

ASA 3000

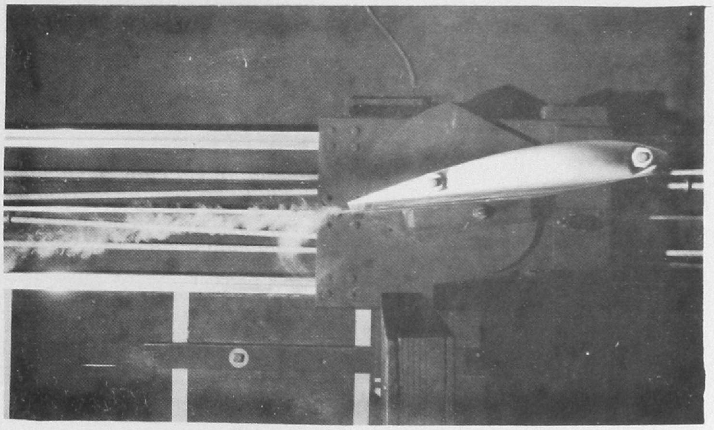

<u>Fig. 8b</u>

Foil Velocity V = 10.8 ft/sec
Distance of Gust Nozzle 6"
Smoke from pressure face

ASA 3000

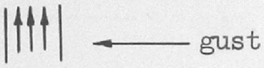

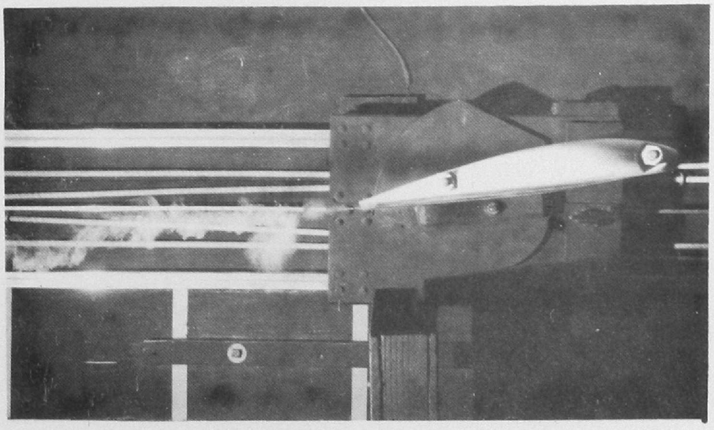

<u>Fig. 8c</u>

Foil Velocity V = 10.8 ft/sec
Distance of Gust Nozzle 6"
Smoke from pressure face

ASA 3000

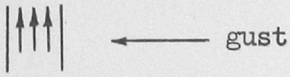

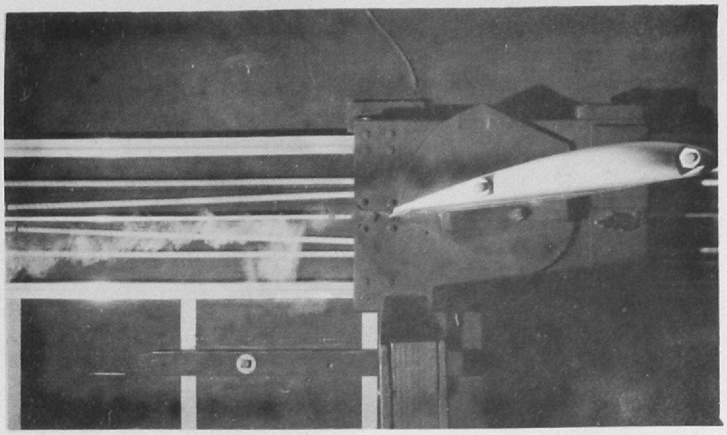

Fig. 8d

Foil Velocity V = 10.8 ft/sec
Distance of Gust Nozzle 6"
Smoke from pressure face

ASA 3000 ← gust

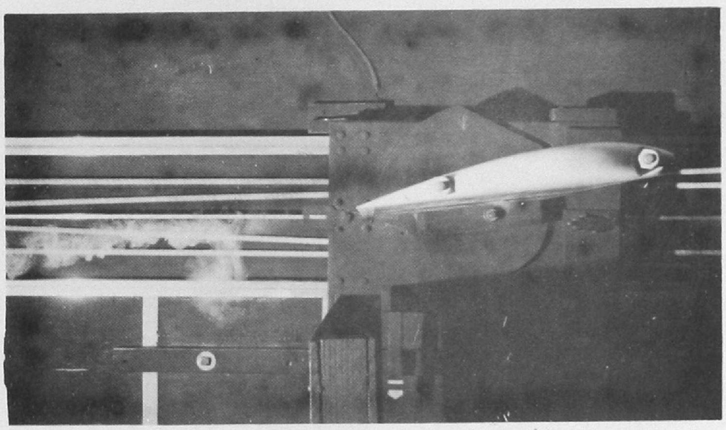

Fig. 8e

Foil Velocity V = 10.8 ft/sec
Distance of Gust Nozzle 6"
Smoke from pressure face

ASA 3000 ← gust

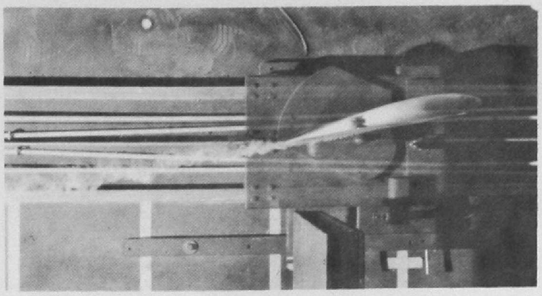

9a No Gust

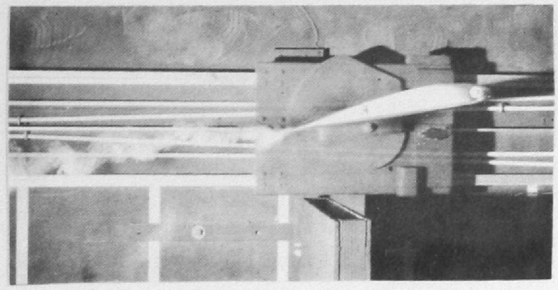

9b |↑↑↑| ← gust

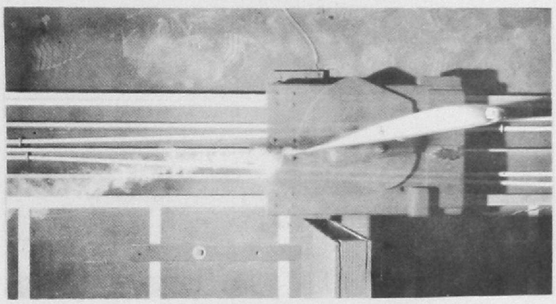

9c |↑↑↑| ← gust

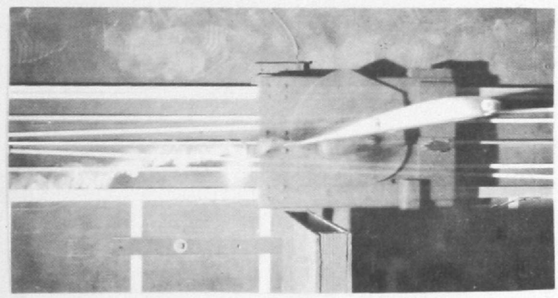

9d |↑↑↑| ← gust

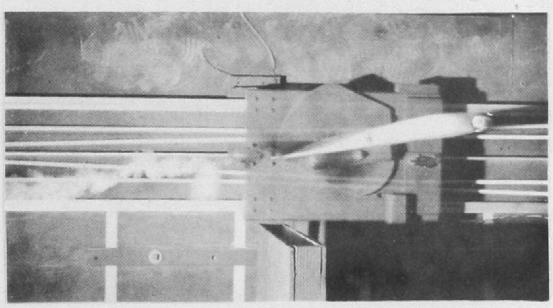

9e |↑↑↑| ← gust

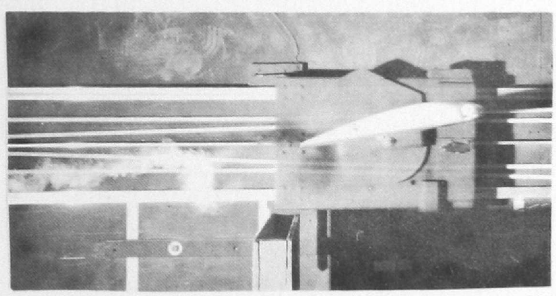

9f |↑↑↑| ← gust

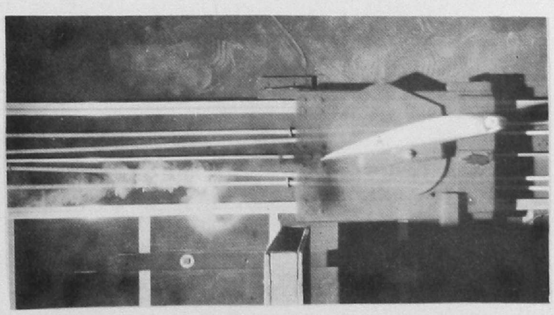

9g |↑↑↑| ← gust

Fig. 9

Foil Velocity V = 10.8 ft/sec
Distance of Gust Nozzle 6"
Smoke from pressure face
ASA 3000

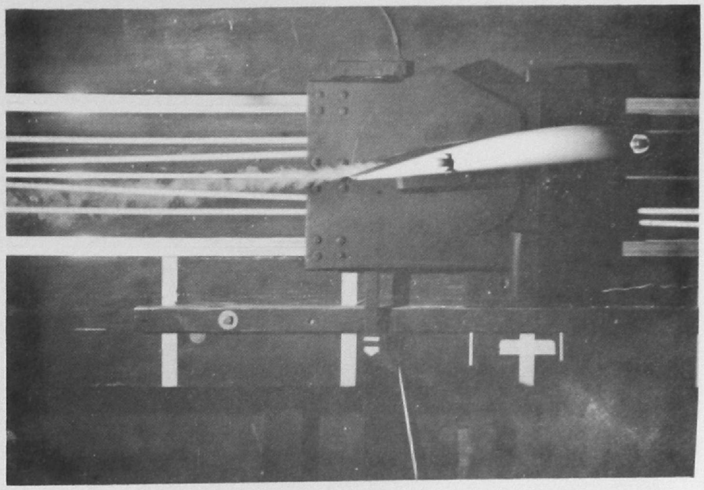

Fig. 10a

Foil Velocity V = 18.89 ft/sec
No Gust
Smoke from suction face

ASA 200

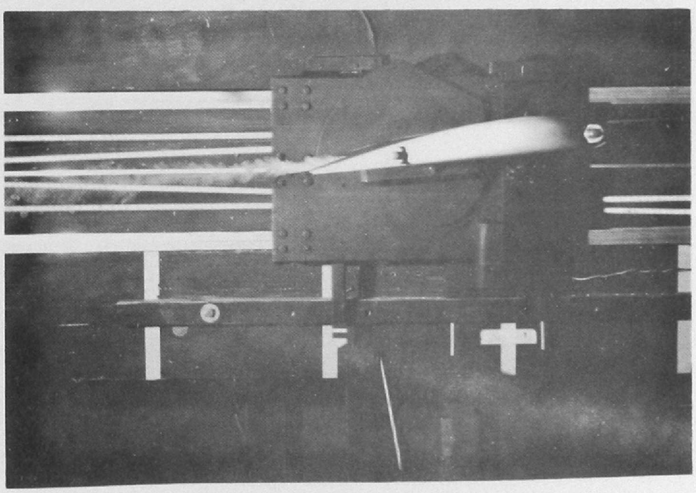

Fig. 10b

Foil Velocity V = 18.89 ft/sec
Distance of Gust Nozzle 12"
Smoke from suction face
Max Gust Velocity 10.13 ft/sec

ASA 200

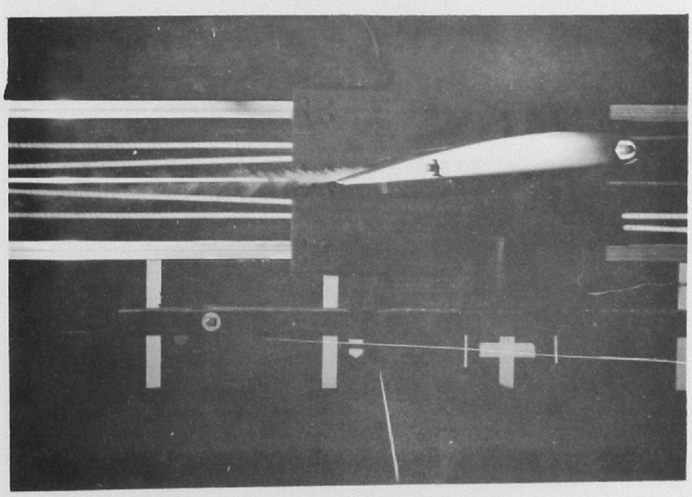

Fig. 10c

Foil Velocity V = 18.89 ft/sec
Distance of Gust Nozzle 12"
Smoke from suction face
Max Gust Velocity 10.13 ft/sec

ASA 200

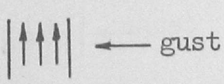

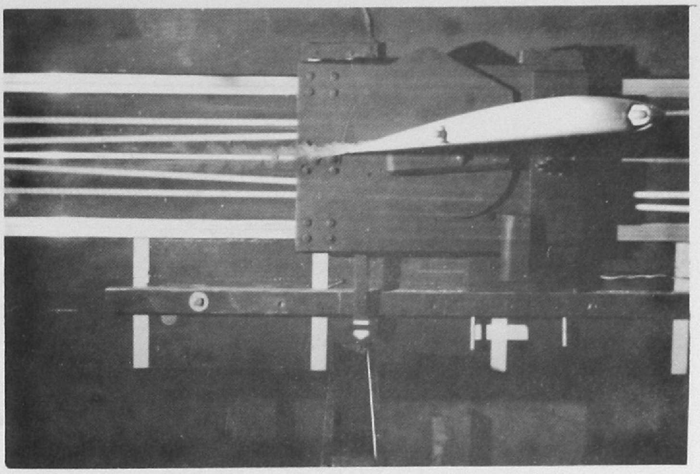

ASA 200 ← gust

Fig. 10d

Foil Velocity V = 18.89 ft/sec
Distance of Gust Nozzle 12"
Smoke from suction face
Max Gust Velocity 10.13 ft/sec

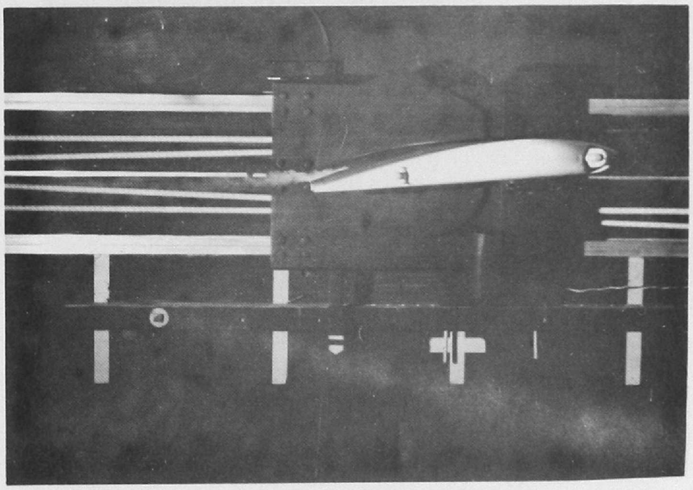

ASA 200 ← gust

Fig. 10e

Foil Velocity V = 18.89 ft/sec
Distance of Gust Nozzle 12"
Smoke from suction face
Max Gust Velocity 10.13 ft/sec

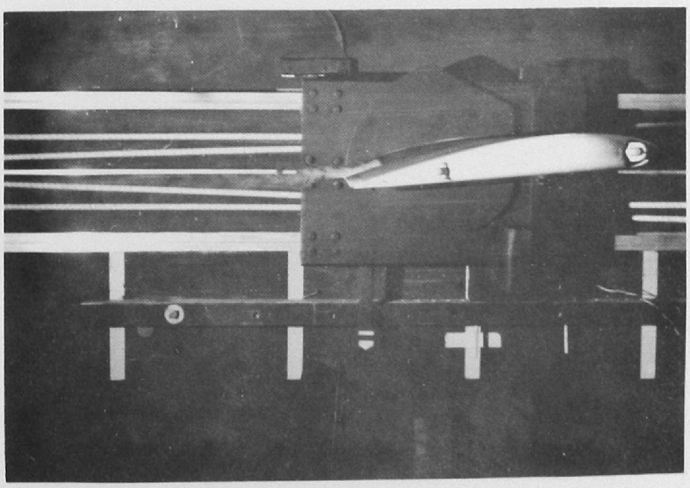

ASA 200 ← gust

Fig. 10f

Foil Velocity V = 18.89 ft/sec
Distance of Gust Nozzle 12"
Smoke from suction face
Max Gust Velocity 10.13 ft/sec

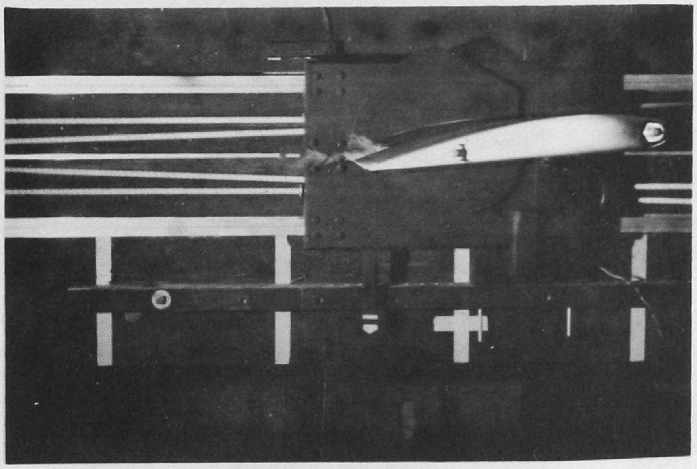

Fig. 10g

Foil Velocity V = 18.89 ft/sec
Distance of Gust Nozzle 12"
Smoke from suction face
Max Crust Velocity 10.13 ft/sec

ASA 200 |↑↑↑| ← gust

(Note the influence of the gust on suction face)

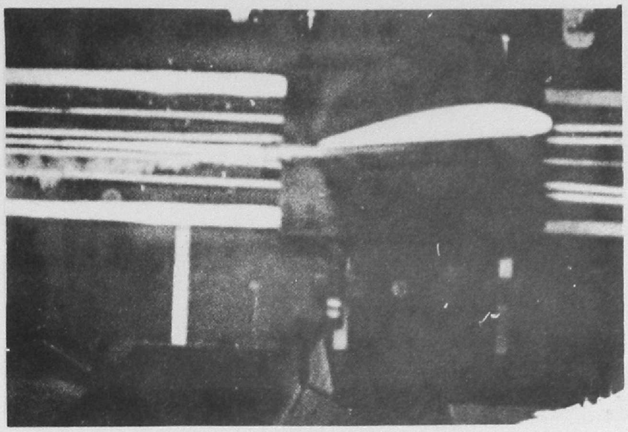

11a gust

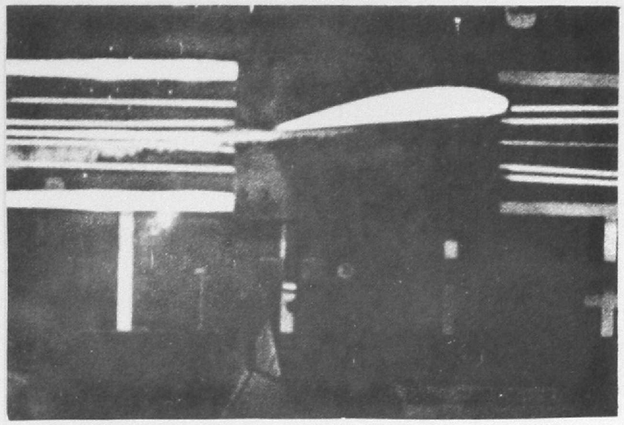

11b gust

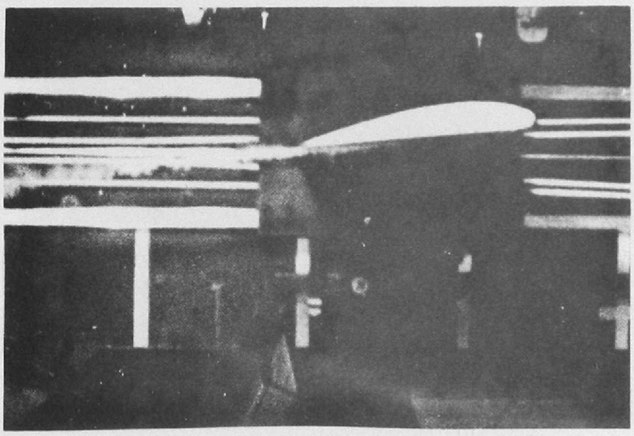

11c gust

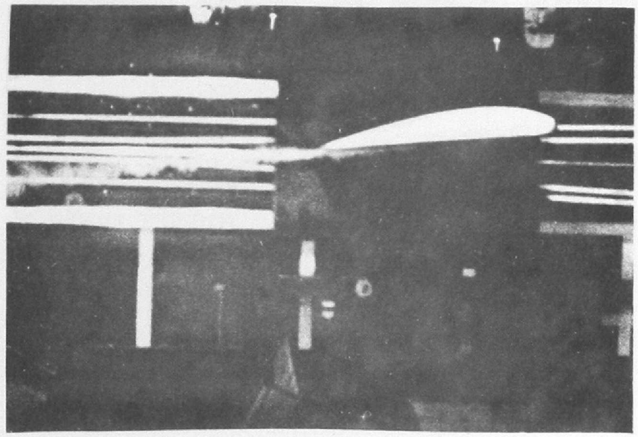

11d gust

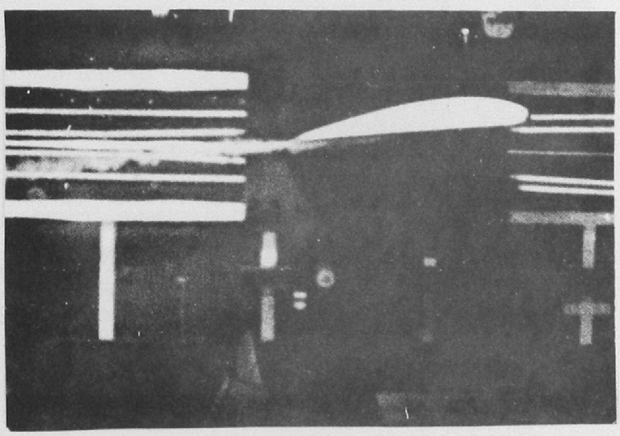

11e gust

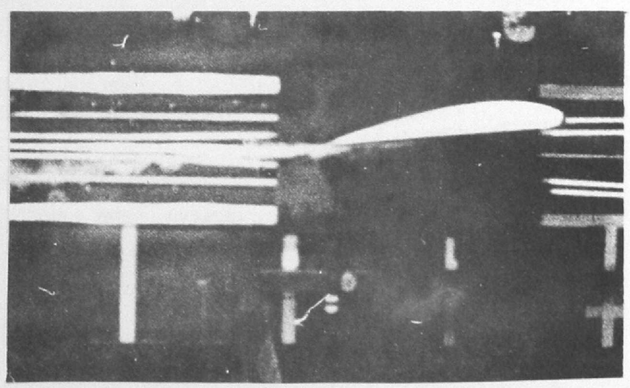

11f gust

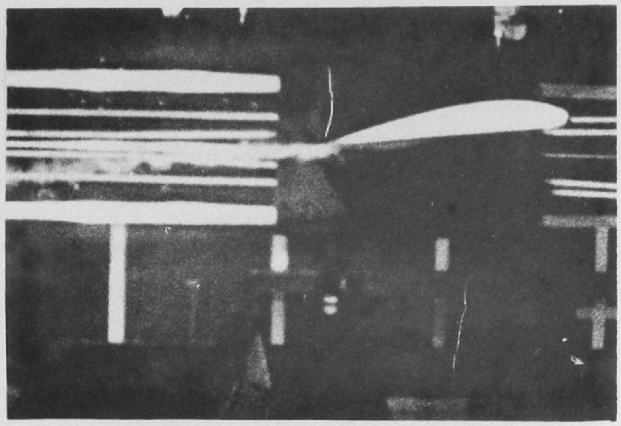

11g gust

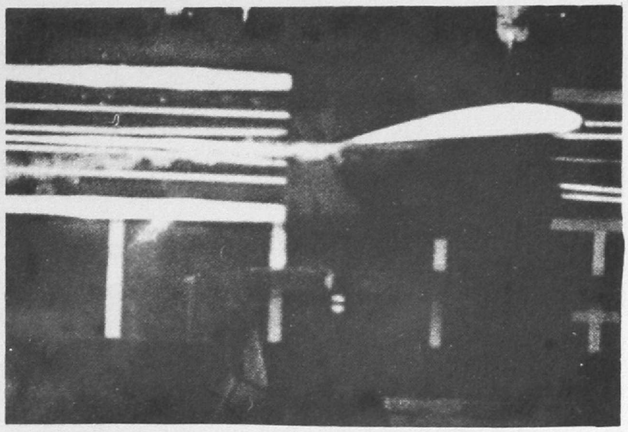

11h gust

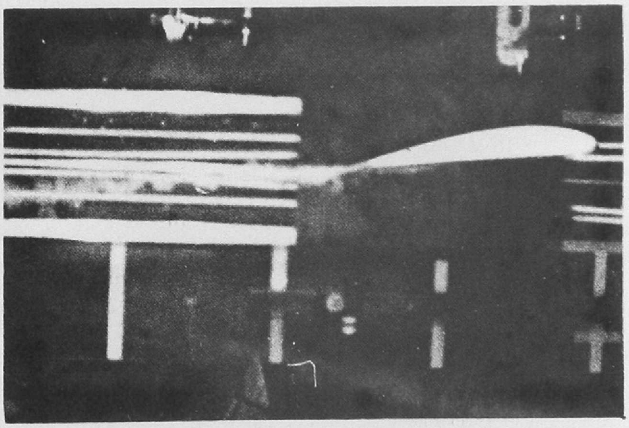

11i gust

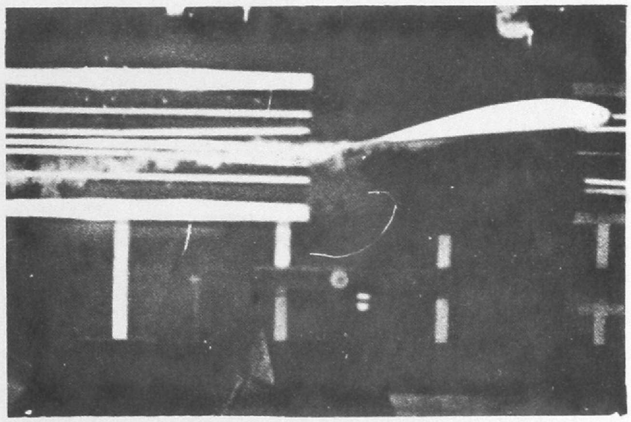

11j gust

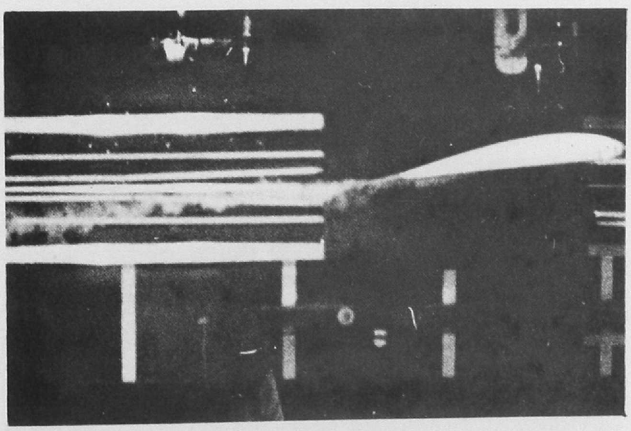

11k gust

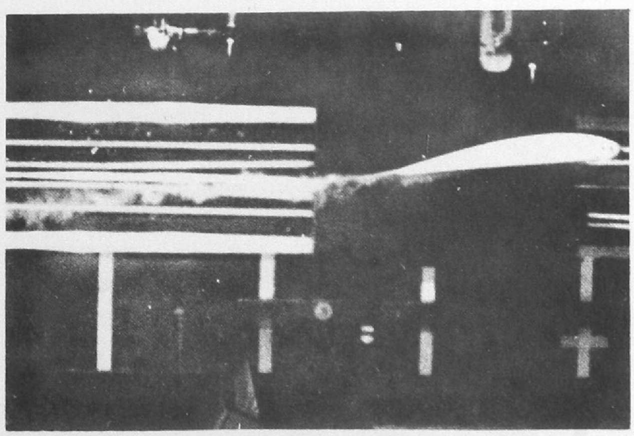

11ℓ gust

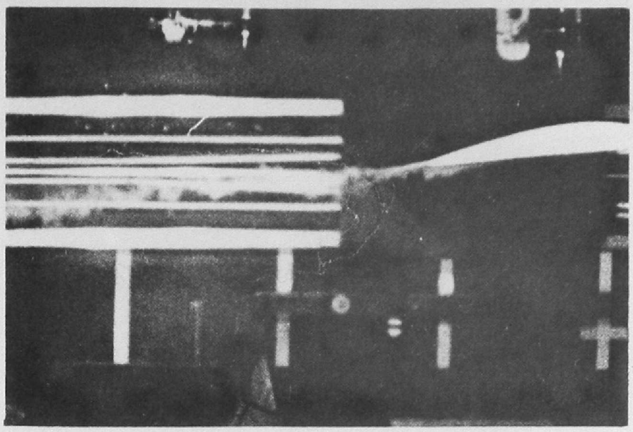

11m ///↑↑/ ← gust

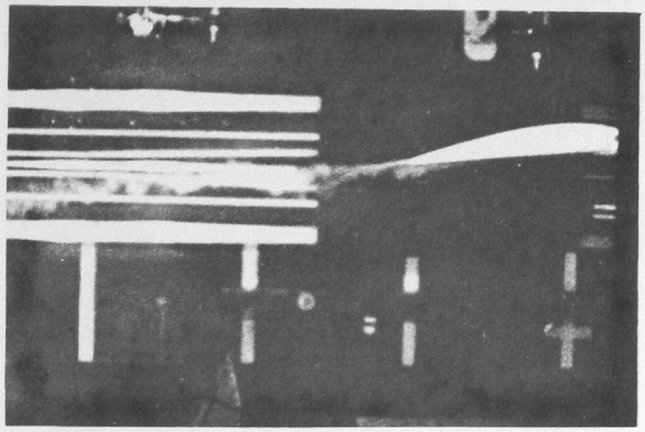

11n ///↑↑/ ← gust

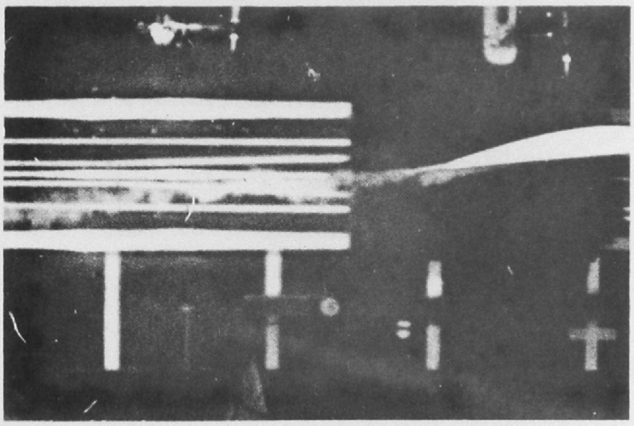

11o ///↑↑/ ← gust

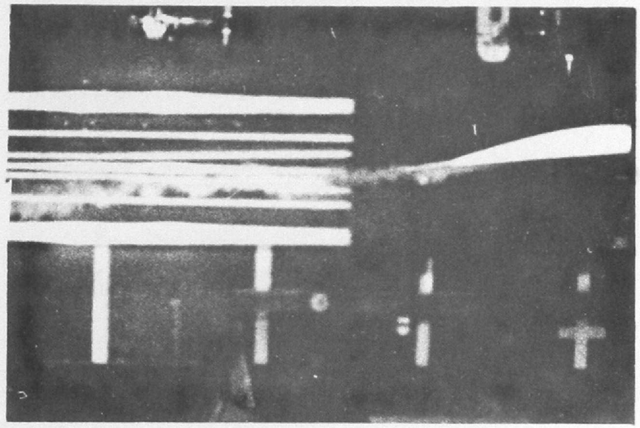

11p ///↑↑/ ← gust

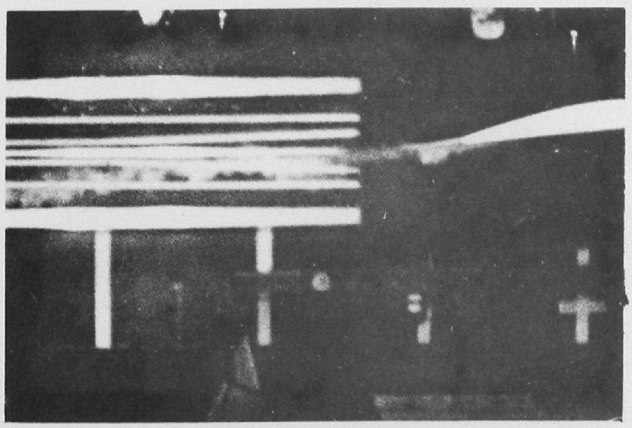

11q ///↑↑/ ← gust

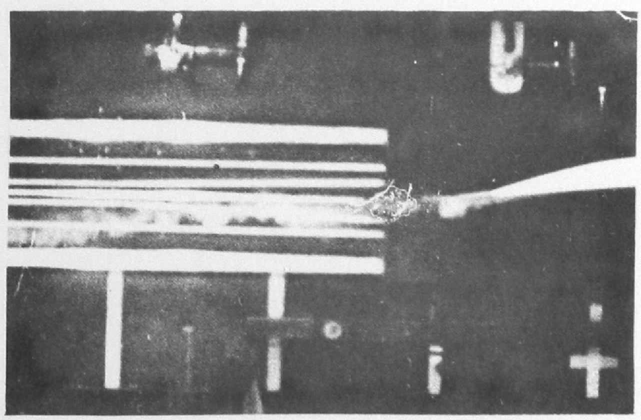

11r ///↑↑/ ← gust

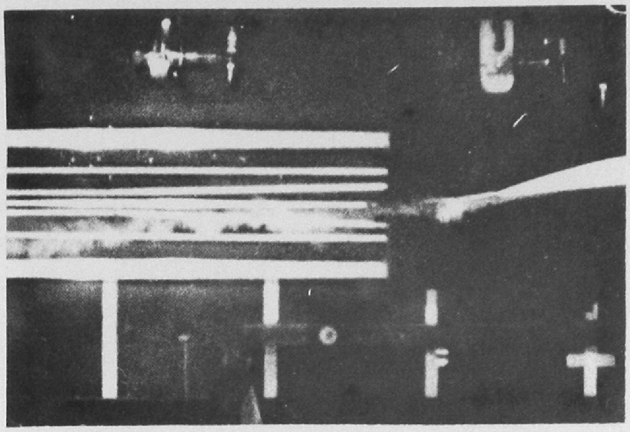

11s /↑↑/ ← gust

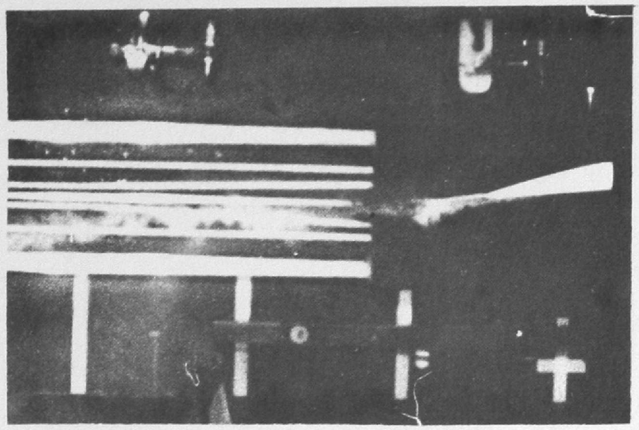

11t /↑↑/ ← gust

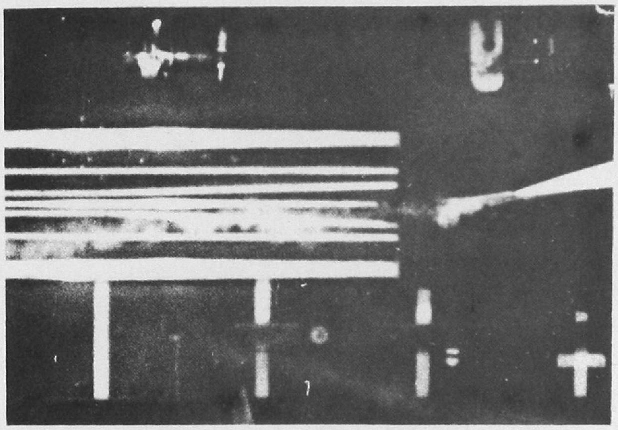

11u /↑↑/ ← gust

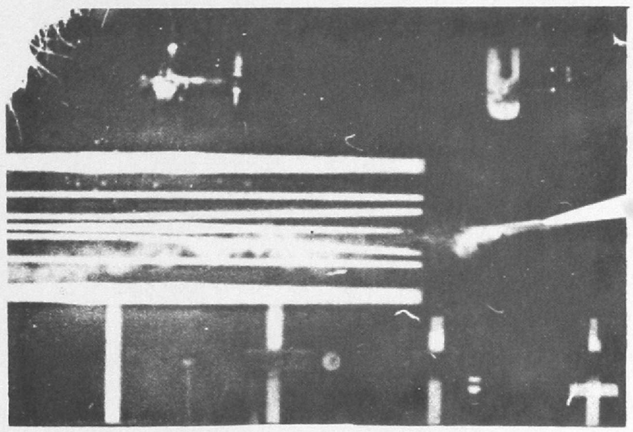

11v /↑↑/ ← gust

Fig. 11

Foil Speed V = 22.9 ft/sec
Distance of Gust Nozzle 12"
Smoke from pressure face
Max Gust Velocity 10.13 ft/sec
Angle of Attack 4.5°
Movie Camera Speed 1260 frames/sec

case of the nozzle being 12" away from the foil face, the gust was approximately six inches wide with a typical measured velocity distribution shown in Fig. 7.

B. Procedure for Photographic Work

The first pictures obtained were taken with a Polaroid camera employing high speed film (ASA numbers between 200 and 3000). In a darkened room, a stroke flash was used with a flash duration of approximately one twelve hundreths of a second. With the camera mounted firmly above the track (three feet above the top of the foil), photos were taken looking directly down along the trailing edge of the foil as it passed. The camera shutter was held open while the strobe flash activated by a trip switch, provided the necessary light and timing. Since the switch could be moved in one inch intervals along the track in the vicinity of the gust source, a sequence of pictures of the flow was made by taking one run per picture. Repeatability was found to be excellent and we are confident as to the accuracy of the sequences recorded.

The next phase of photographic study was to take moving pictures with a medium speed camera. Using high speed film at about 300 frames per second, the clarity of these first movies was fairly good.

The third and last phase of picture taking involved the use of a very high speed ("Fastax") movie camera. Unfortunately, the pictures turned out rather grainy as they were run at approximately 1260 frames per second using very high speed film. The relative clarity of the earlier work was not matched with these last attempts.

V. CONCLUSIONS AND RECOMMENDATIONS

The pictures taken of the flow patterns around the trailing edge of a foil passing through a narrow gust indicates that the mathematical artifice of the Kutta conditions does not satisfactorily represent the physical model. It is therefore likely that an improved mathematical model must be found before we can predict theoretically the lift and moment acting on the foil as a function of position in the gust. No such mathematical model is proposed at this time. It is hoped, however, that the flow patterns presented here may come to indicate what physical features must be revealed by an theoretical treatment.

The present study was undertaken on very limited funding and was primarily conceived as a pilot program to develop experimental techniques and in so doing get a preliminary look at the flow. In this respect it has been successful. As expected, however, it leaves many of the old questions unanswered and presents some nagging new ones. This research should therefore be continued on a much broader basis than has been the case so far.

As an immediate extension of the flow visualization study it is suggested that the time varying pressure distributions around the foil be measured directly on the foil, and the lift and drag calculated from these distributions by simple integration. Hopefully a project with this objective in mind can be undertaken.

It should be pointed out that the experimental setup of the present study permits the introduction of several gusts spaced down the track. These may be blowing air across the foil path from either side.

VI. REFERENCES

1. Abbott, I. H. and Doenhoff, A. E., Theory of Wing Sections, Dover Publications, 1958.

2. von Karman, Th. and Sears, W. R., "Airfoil Theory for Non-Uniform Motion," Journal of Aeronautical Sciences, Vol. 5, No. 10, Aug. 1938.

3. Durand, W. F., Aerodynamic Theory, Vol. 11, Div. E, J. Springer Verlag, 1935.

4. Meyer, R. X., "Interference Due to Viscous Wakes between Stationary and Rotating Blades in Turbomachines," Doctoral Thesis, John Hopkins University, 1955.

5. Pinkerton, R. M., "Calculated and Measured Pressure Distributions over the Midspan Section of the NACA 4412 Airfoil," NACA Report No. 563, 1936.

VII. APPENDIX

The problem of unsteady flow about an airfoil has been treated by such authors as Wagner, Kussner, Theodorsen, von Karman, Sears, and others. Most of the work done in this area has been based on two dimensional thin airfoil theory. The results of von Karman and Sears (Reference 2) appear to be applicable in this case unless the width of the gust is of the order or smaller than the chord length of the foil. This happens to be the case that concerns this report. In an effort to extend the basic theory developed in Reference 2 to this case Bruce Nelson started from the basic equations and developed a thin airfoil theory for the problem. The following is an abbreviated summary of the solution.

Munks integral formulae (see Reference 3) were used to calculate the lift and moment functions. These formulae are subject to the same limitations as the Fourier series formulae used in Reference 2 and were used because they appeared to be more natural for the problem.

The coordinate system used was the same as in Reference 2, with the chord length non-dimensionalized to two, the width of the gust as a, the foil velocity as U, and the gust velocity as V. The angles defining the intersection of the edges of the gust and the foil are θ_o and β_o (see Fig. A-1 below).

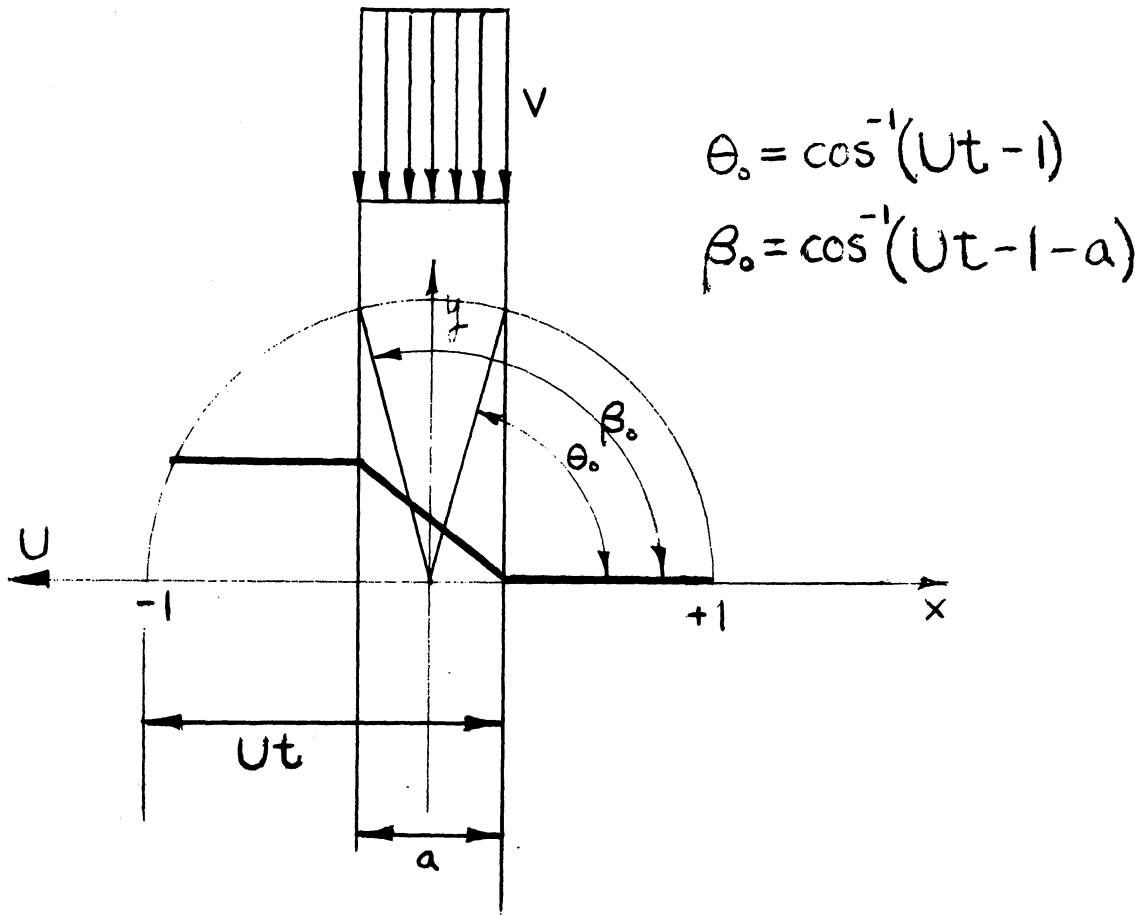

<u>Fig. A-1</u>

Definition of Angles θ_o and β_o

The "broken line" airfoil technique leads to four distinct regions for this problem, as opposed to only two in Reference (2). They are as follows.

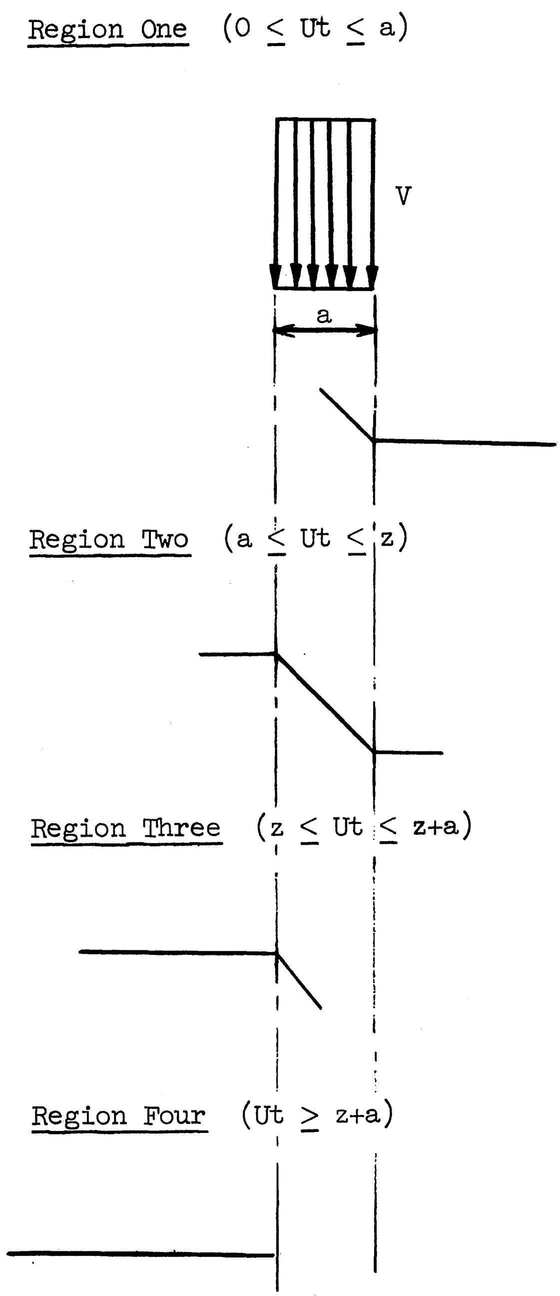

Fig. A-2

Four Regions of the Problem for the "Broken Line Airfoil"

Under the transformation $x = \cos\Theta$, the formulae which arise are as follows:

$$\Gamma_o = -U \int_0^{2\pi} \frac{dy}{dx}(1 + \cos\tau)\, d\tau$$

where,

$$\frac{dy}{dx} = \text{slope of the broken line airfoil}$$

$$\gamma_o = \frac{-U}{\pi \sin\Theta} \int_0^{2\pi} \frac{dy}{dx} \cot\frac{\Theta - \tau}{2} \sin\tau\, d\tau + \frac{\Gamma_o}{\pi \sin\Theta}$$

The lift is given by

$$L = L_o + L_1 + L_2 = \text{LIFT}$$

with

$$L_o = \rho U \Gamma_o$$

$$L_1 = -\rho\left(\frac{d}{dt}\right) \int_{-1}^{1} \gamma_o(x)x\,dx = \frac{\rho}{2} \left(\frac{d}{dt}\right) \int_{\pi}^{0} \gamma_o(\Theta) \cos\Theta \sin\Theta\, d\Theta$$

$$L_2 = \rho U \int_1^{\infty} \gamma(\xi) \sqrt{\xi^2 - 1}\, d\xi$$

Similarly

$$M = M_o + M_1 + M_2 = \text{MOMENT}$$

with

$$M_o = -\rho U \int_{\pi}^{0} \gamma_o(\Theta) \cos\Theta \sin\Theta\, d\Theta$$

$$M_1 = -\frac{1}{2}\left(\frac{d}{dt}\right)\int_{-1}^{1} \gamma_o(x)\left[x^2 - \frac{1}{2}\right] dx = \frac{1}{4}\left(\frac{d}{dt}\right)\int_{\pi}^{o} \gamma_o(\Theta) \cos 2\Theta \sin \Theta \, d\Theta$$

$$M_2 = \frac{-L_2}{2}$$

Upon completion of the indicated integration we find that the lift and moment are given as follows. (Superscripts refer to regions.)

Region One

$$L_o^{(1)} + L_1^{(1)} = UV[\pi - \Theta_o] = 2\rho UV \cos^{-1}(1 - Ut)$$

$$M_o^{(1)} + M_1^{(1)} = \rho UV[\Theta_o - \pi] = -\rho UV \cos^{-1}(1 - Ut)$$

Region Two

$$L_o^{(2)} + L_1^{(2)} = \rho UV[\beta_o - \Theta_o]$$

$$M_o^{(2)} + M_1^{(2)} = \rho UV[\Theta_o - \beta_o]$$

Region Three

$$L_o^{(3)} + L_1^{(3)} = 2\rho UV\beta_o$$

$$M_o^{(3)} + M_1^{(3)} = -\rho UV\beta_o$$

Region Four

$$L_o^{(4)} + L_1^{(4)} = 0$$

$$M_o^{(4)} + M_1^{(4)} = 0$$

At this point one can see that since the L_2 term of the lift always acts at the quarter chord point, the total lift acts at the quarter chord point at all times (see results for lift and moment above). Although this result is arrived at in Reference (2), it is quite surprising and disappointing that this result should hold in Region 2, where the foil is both entering and leaving the gust. It is disappointing because the results obtained above are valid for an infinitesimally small width of the gust, and we know physically that as the ratio of the chord length to the gust width approaches infinity that the lift vector should act at the point of impingement of the gust if the foil has no angle of attack. This inconsistency has been shown earlier by Meyer in a more rigorous manner (Reference 4).

Since thin airfoil theory leads to incorrect results for large chord length to gust width ratios, another approach must be taken in an effort to find the lift and moment functions. A careful study of the pictures taken led the authors to believe that a "flat plate" jet deflection phenomena is perhaps the governing effect when the gust is narrow. This can be illustrated by the following sketch.

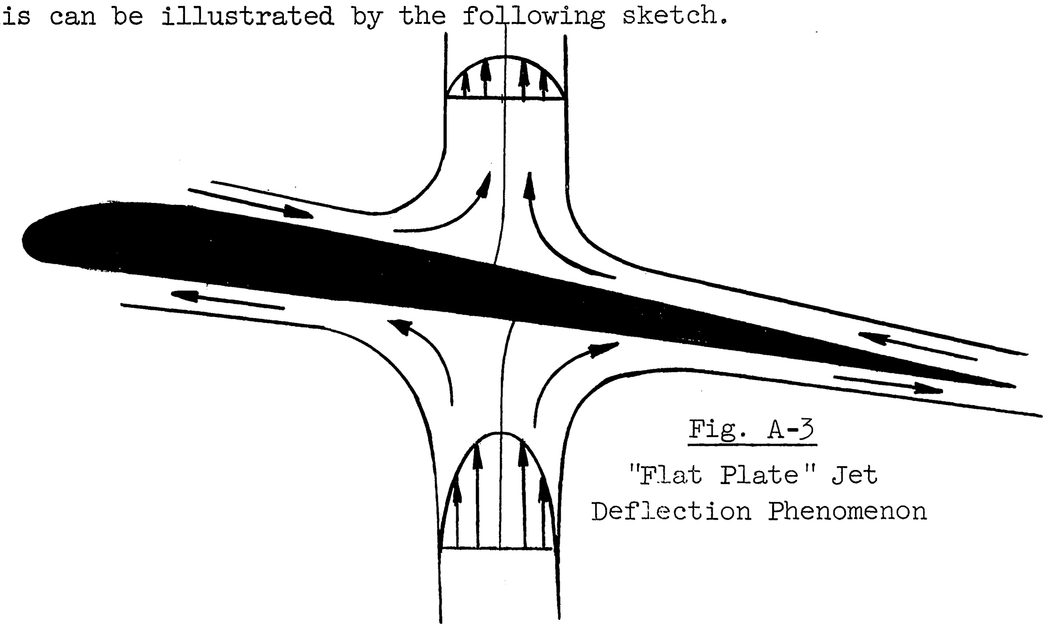

Fig. A-3
"Flat Plate" Jet
Deflection Phenomenon

Although this interpretation of the unsteady flow pattern is crude, momentum can be applied to the above sketch and it should be possible to estimate the additional terms of the lift and moment due to the presence of this gust. The effect on the suction side of the gust velocity distribution is expected to be negligible. It is suggested, however, that further studies be made to ascertain whether this is so, because we may well find that the time variation of the flow on the suction side of the foil as it passes through the gust significantly influences the pressure distribution on that side.